

Comparison of calculated and experimental angle-resolved photoemission spectra from Cu

M. Sagurton*

Department of Physics, State University of New York at Stony Brook, Stony Brook, New York 11794
(Received 21 December 1983; revised manuscript received 2 April 1984)

Experimental angle-resolved photoemission spectra obtained from a Cu(111) surface for $11.8 \leq \hbar\omega \leq 21.2$ eV are analyzed by comparing them with spectra calculated with the parametrized scheme presented in the preceding paper. It is found that the final state can be described in terms of bands with free-electron-like, rather than bulklike, E -versus- \vec{k} dispersions; that the effective inner potential used to calculate these bands can vary with the final-state energy E and emission direction \hat{R} ; that the final state can consist of a mixture of up to several free-electron-like bands; and that momentum broadening can strongly influence peak shapes and positions. The usefulness of the scheme for determining initial-state band positions is demonstrated. It is found that the Fresnel equations are adequate for describing the electric field of the incident light within the solid.

I. INTRODUCTION

Several authors have proposed, on the basis of angle-resolved photoemission (ARP) measurements, precise experimental E -versus- \vec{k} relationships for portions of the occupied bulk bands of Cu.¹⁻⁶ In these works, initial-state band positions have been extracted from experimental spectra by working within a strict direct-transition model. When $E(\vec{k})$ is determined with spectra from a single-crystal face,¹⁻⁴ the Bloch wave vector \vec{k} associated with an observed spectral feature is obtained by assuming that the final states have either bulklike⁴ or free-electron-like¹⁻³ dispersions. In triangulation methods involving spectra from two crystal faces,^{5,6} it is assumed only that the final states lie along bands with dispersions which are crystal face independent.

While the energy bands mapped out with these procedures have agreed well with first-principles band-structure calculations, complications involving the final state can limit their general usefulness. If the assumptions concerning the dispersion of ψ^f become inaccurate, the \vec{k} point at which direct transitions occur can be placed incorrectly; the decay of ψ^f into the bulk results in momentum broadening in the optical matrix element and indirect transitions; and (in the context of a three-step model) surface umklapp processes and propagation in secondary Mahan cones can occur and be difficult to interpret correctly. It is in an attempt to account for such effects in the interpretation of spectra that the calculation of peak intensities and shapes, as well as positions, should be very useful, as these are generally quite sensitive to any proposed behavior for ψ^f , and can thus be used to help determine ψ^f .

In this paper we analyze a selected set of experimental spectra obtained from a Cu(111) surface for $11.8 \leq \hbar\omega \leq 21.2$ eV with calculations performed with the parametrized scheme, based upon a one-step model of photoemission, presented in the preceding paper (hereafter referred to as I). We find, in general agreement with the results of some other workers,⁷ that the final state is

described by bands with free-electron-like dispersions, rather than by bulk bands. We also find, however, that it frequently consists of a mixture of more than one free-electron-like band, occasionally including bands with group velocities directed into rather than out of the bulk; that the inner potential used to calculate these bands can be a function of the emission direction \hat{R} and energy E defining the final state; and that momentum broadening can strongly influence peak shapes and positions.

The determination of initial-state band positions with the present scheme is demonstrated. It is found that such determinations are only feasible when the final state is relatively simple and consists of a small number of single-OPW bands.

II. EXPERIMENT

Experiments were performed with a Vacuum Generators ADES 400 electron spectrometer. A Cu(111) single crystal was prepared using standard techniques. The angular acceptance of the hemispherical analyzer was $\pm 2^\circ$, and spectra were collected with an energy resolution of 0.15 eV full width at half maximum (FWHM). The experimental geometry was such that the emission direction, the photon wave vector, and the surface normal all lay in the horizontal plane. We let θ and ψ represent the emission angle and the angle of incidence of the light, respectively, with respect to the surface normal. θ is defined so as to increase toward the nine o'clock position on the sample surface, while ψ increases in the opposite direction. The azimuthal orientation of the crystal was determined with LEED and will be specified by an angle ϕ , defined as the clockwise rotation needed to bring the $[2\bar{1}\bar{1}]$ direction to the nine o'clock position. Radiation at energies of 11.8, 16.9, and 21.2 eV was obtained with a high-intensity discharge lamp designed by Shevchik.⁸ For $\hbar\omega = 11.8$ and 16.9 eV the incident light was polarized by double reflection from two gold mirrors. Unfortunately, the efficiency of the polarizer was found to decrease substantially with increasing photon energy. The degree of polarization, defined by⁹

$$P = \left| \frac{I_s - I_p}{I_s + I_p} \right|, \quad (1)$$

where I_s (I_p) denotes the relative intensity of the s - (p -) polarized component of the light, was $\cong 0.9$ for $\hbar\omega = 11.8$ eV, but only $\cong 0.65$ for $\hbar\omega = 16.9$ eV. We let χ represent the orientation of the electric field vector for polarized light, with $\chi = 0^\circ$ (90°) corresponding to s - (p -) polarized light.

III. RESULTS

A. Determination of parameters

Following I, our result for the optical matrix element connecting an initial Bloch state $\psi_{\vec{k}}^i$ with a given OPW component of the final state involves an expression $(\vec{E}_{\parallel} + \alpha_E(\psi)E_{\perp}\hat{\chi}) \cdot \vec{P}^i$, where E_{\parallel} and E_{\perp} are the parallel and perpendicular components, respectively, of the electric field in vacuum, and \vec{P}^i is of the form

$$\begin{aligned} \vec{P}^i = & [A_{xz}^i + \alpha_p j_1(k^i R_{MT}) A_x^i] \hat{x} + [A_{yz}^i + \alpha_p j_1(k^i R_{MT}) A_y^i] \hat{y} \\ & + \{ \xi_d A_{3z^2-r^2}^i + \alpha_p j_1(k^i R_{MT}) \xi_p A_z^i \\ & + \alpha_s [j_0(k^i R_{MT}) + \beta_s] A_{i,0}^i \} \hat{z}, \end{aligned} \quad (2)$$

where the A^i are the amplitudes of the various angular momentum components of the initial state within a muffin-tin sphere.

As the parameters ξ_d , ξ_p , α_p , α_s , and β_s are assumed to be independent both of the initial-state energy E^i , for spectra obtained with a given photon energy, and the emission direction \hat{R} , they were chosen for each photon energy so as to maximize the average agreement obtained, over all the emission directions sampled, between the calculated and experimental spectra. The main contribution to the photocurrent from Cu is from the d component of the band structure. Since, in the calculation, this contribution depends only on the value of ξ_d , and since the cal-

culated relative peak intensities in many spectra are found to be sensitive to ξ_d , it is straightforward in practice to fit this parameter to experiment. For $\hbar\omega = 11.8, 16.9$, and 21.2 eV, we obtained $\xi_d = -0.8, -1.0$, and -1.3 , respectively. In contrast to an assumption made in previous works,^{10,11} but consistent with first-principles calculations by Jepsen¹² for $\hbar\omega = 16.9$ eV, these results indicate that the $d \rightarrow f$ cross section is larger than the $d \rightarrow p$ cross section at these photon energies. They furthermore indicate that the relative strength of the $d \rightarrow f$ excitation channel is an increasing function of the photon energy.

The calculated photocurrent from the s - p component of the band structure is dependent upon the parameters ξ_p , α_p , α_s , and β_s . As the s - p -derived photocurrent was significant in only a relatively small number of spectra, however, these parameters were underdetermined by our experimental results. It was found that the calculated spectra were not very sensitive to β_s , so β_s was simply set equal to zero. ξ_p was assigned the value -1.0 , which fixes the amplitude of the $p \rightarrow d$ excitation channel at twice that of the $p \rightarrow s$ channel. The values then obtained for α_p and α_s by fitting to the experimental results were -0.8 and -0.7 , respectively, for $\hbar\omega = 11.8$ eV, and -0.5 and -0.4 for $\hbar\omega = 16.9$ eV. The relative magnitudes of α_p and α_s are also uncertain, however, as α_s can be increased at the expense of α_p , or vice versa, and roughly equivalent agreement between the theoretical and experimental spectra is obtained.

$\alpha_E(\psi)$, the scaling factor for the normal component of the electric field within the solid, was chosen for each spectrum so as to maximize the agreement with experiment. Although this parameter is in principle complex, the calculated peak intensities were found not to be very sensitive to its phase, and so it was treated as being real. The results obtained are discussed in Sec. IV.

The remaining parameters enter into the description of the final-state wave function $\psi_{\vec{R},E}^d$, where \hat{R} defines the emission direction and E is the final-state energy. Following I, we have

$$\begin{aligned} \psi_{\vec{R},E}^d(\vec{r}) = & e^{-\Gamma(\hat{R},E)z} \sum_{\vec{G}_s} \{ f_{\vec{R},E}^+(\vec{G}_s) e^{-\Gamma_{\vec{R},E}^+(\vec{G}_s)z} \langle \vec{r} | \text{OPW}[\vec{K}^+(E, \vec{k}_s + \vec{G}_s)] \rangle \\ & + f_{\vec{R},E}^-(\vec{G}_s) e^{-\Gamma_{\vec{R},E}^-(\vec{G}_s)z} \langle \vec{r} | \text{OPW}[\vec{K}^-(E, \vec{k}_s + \vec{G}_s)] \rangle \}, \end{aligned} \quad (3)$$

where \vec{k}_s is the wave vector which characterizes $\psi_{\vec{R},E}^d$ in the surface Brillouin zone, $\vec{K}^{\pm}(E, \vec{k}_s + \vec{G}_s)$ are wave vectors with parallel components $\vec{k}_s + \vec{G}_s$ and z components given by

$$K_z^{\pm}(E, \vec{k}_s + \vec{G}_s) = \pm \left[\frac{2m}{\hbar^2} [E + \Phi(\hat{R}, E)] - |\vec{k}_s + \vec{G}_s|^2 \right]^{1/2} \quad (4)$$

(where $E=0$ is the vacuum level), and the sum is over the surface reciprocal-lattice vectors \vec{G}_s corresponding to real

K_z^{\pm} . It was in general assumed that the decay constants $\Gamma(\hat{R}, E)$ and $\Gamma_{\vec{R},E}^{\pm}(\vec{G}_s)$, the OPW amplitudes $f_{\vec{R},E}^{\pm}(\vec{G}_s)$, and the inner potential $\Phi(\hat{R}, E)$, were independent of E over the range of final-state energies (≤ 5 eV) relevant to any given photoemission spectrum. When this assumption is not reasonably accurate, an attempt to fit these quantities to the experimental results becomes much more uncertain. Typically, calculated spectra were found to be very sensitive to the values of the OPW amplitudes $f_{\vec{R},E}^{\pm}(\vec{G}_s)$, but not very sensitive to the values of the decay constants $\Gamma(\hat{R}, E)$ and $\Gamma_{\vec{R},E}^{\pm}(\vec{G}_s)$. An estimate for $\Phi(\hat{R}, E)$

can be obtained by adding Burdick's theoretical value of 7.5 eV for the energy difference between the muffin-tin zero and the Fermi level¹³ to the 5.0-eV work function of Cu. Except where stated otherwise, $\Phi(\hat{R}, E) = 12.5$ eV was used in the calculations. It was found, however, that the calculated spectra were not generally very sensitive to changes in $\Phi(\hat{R}, E)$ of a few tenths of an electron volt.

B. Comparison of calculated and experimental spectra

In this section we analyze a selected set of experimental spectra by comparing them with corresponding calculated results. All calculated spectra were convoluted with a Gaussian energy broadening function of FWHM 0.35 eV in order to simulate hole lifetime and experimental broadening effects. However, no provision was made for the nonzero angular acceptance of the analyzer, or, in the case of spectra obtained with polarized light, for the fact that the degree of polarization was less than unity (Sec. II). The initial-state energies and wave functions were computed with Smith and Mattheiss' version of the combined interpolation scheme,¹⁴ using the parameters obtained by these authors from a least-squares fit to the APW band structure of Burdick.

In the figures which follow, calculated and experimental ARP spectra are shown together with the subset of the initial-state band structure which can contribute to the spectra via \vec{k}_s conserving optical transitions. Thus, the bands are plotted in such a way that for any initial-state energy E^i , \vec{k}_{\parallel} is given by

$$\vec{k}_{\parallel} = \{ [2m(E^i + \hbar\omega)]^{1/2} / \hbar \} \hat{R}_{\parallel} + \vec{G}_s, \quad (5)$$

for some \vec{G}_s (when E^i is measured with respect to the vacuum level). \vec{k}_{\parallel} is therefore in general a function of E^i . Also shown on the band-structure plots, shifted down by the photon energy $\hbar\omega$, are the free-electron-like E -versus- \vec{k} dispersions of the OPW "bands" which appear in Eq. (3). These bands intersect the initial-state bands at "direct-transition points" (DTP's), where \vec{k} -conserving optical transitions can occur.

For simplicity, the OPW wave vectors $\vec{K}^{\pm}(E, \vec{k}_s + \vec{G}_s)$ will henceforth be denoted as \vec{K}_n^{\pm} , where each value of n is associated with a particular \vec{G}_s . Similarly, the amplitudes $f_{\vec{R}, E}^{\pm}(\vec{G}_s)$ will be denoted f_n^{\pm} . \vec{K}_1^{-} will always denote the wave vector of that plane wave $\exp(i\vec{K}_n^{-} \cdot \vec{r})$ which, after refraction at a surface between vacuum and a potential well of magnitude Φ , propagates in the direction \hat{R} of the detector.

1. $\hbar\omega = 16.9$ eV, $\theta = 0^\circ$

Normal photoemission from Cu(111) has been studied by several workers.^{4,10,11,15-20} In Fig. 1 we show experimental spectra taken with p -polarized light ($\chi = 90^\circ$) at angles of incidence $\psi = 75^\circ$ and 45° , and a spectrum taken with s -polarized light. The peaks at -3.85 and -2.7 eV are due to transitions from the Λ_1 band and the higher-energy doubly degenerate Λ_3 bands, respectively. Also shown, as the solid curves, are theoretical spectra computed

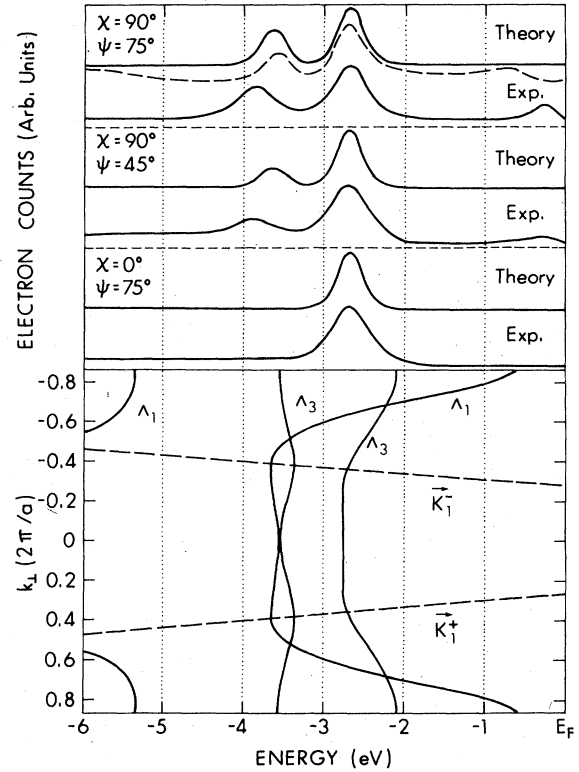


FIG. 1. Calculated and experimental ARP spectra for $\hbar\omega = 16.9$ eV and $\theta = 0^\circ$. The dashed curve was computed with $\alpha_p = 6.0$, $\Gamma = 0.1(2\pi/a)$, and $\alpha_E = 0.19$.

ed with the final state

$$\psi^f(\vec{r}) = e^{-0.03z} \langle \vec{r} | \text{OPW}(\vec{K}_1^-) \rangle, \quad (6)$$

where the decay constant Γ is in units of $2\pi/a$.

Our model for the final state [Eq. (3)] contains two OPW components for this photon energy and emission direction, $|\text{OPW}(\vec{K}_1^-)\rangle$ and $|\text{OPW}(\vec{K}_1^+)\rangle$ (Fig. 1). However, due to the symmetry properties of states on the Λ axis, the shape of calculated spectra is independent of the relative amplitudes f_1^+ and f_1^- of $|\text{OPW}(\vec{K}_1^+)\rangle$ and $|\text{OPW}(\vec{K}_1^-)\rangle$ in ψ^f (for reasonably small values of Γ), and so it is not possible to determine f_1^+ and f_1^- by comparing calculated and experimental spectra.

There is good agreement between the predicted and observed positions of the peak from the Λ_3 bands; however, the predicted position of the peak from the Λ_1 band is in error by 0.25 eV. This discrepancy cannot be removed by adjusting the inner potential, since the DTP is at the band minimum for the assumed value of 12.5 eV. Assigning it to an error in the position of the Λ_1 band places this band at -3.85 eV at the DTP, a result which agrees well with the Korringa-Kohn-Rostoker (KKR) band-structure calculations of Janak *et al.*,²¹ and with previous experimental determinations.⁴

For $\chi = 90^\circ$, the calculated relative intensity of the peak from the Λ_1 band is very sensitive to $\alpha_E(\psi)$. The values which gave the best agreement with experiment (as shown in Fig. 1) were 0.45 for $\psi = 45^\circ$, and 0.17 for $\psi = 75^\circ$, con-

firming previous indications¹⁹ that it is very important to account for refraction effects in a calculation of peak intensities when the incident light is p polarized. A source of uncertainty in these values for α_E is the fact that the DTP on the Λ_1 band occurs near the band minimum, so that relatively small errors in the position of the DTP could have a significant effect on the predicted relative peak intensities, due to initial one-dimensional density-of-states effects. In addition, the relative peak intensities depend on ξ_d as well as α_E , so that some cancellation of errors could occur. It is useful, therefore, to consider the ψ dependence of the ratio of the intensities of the peaks from the Λ_1 and Λ_3 bands. Denoting this ratio $R_{\Lambda_1/\Lambda_3}(\psi)$, we have

$$R_{\Lambda_1/\Lambda_3}(\psi) \propto [\alpha_E(\psi)E_{\perp}(\psi)/E_{\parallel}(\psi)]^2 = [\alpha_E(\psi)\tan\psi]^2, \quad (7)$$

which implies that

$$R_{\Lambda_1/\Lambda_3}(75^\circ)/R_{\Lambda_1/\Lambda_3}(45^\circ) = 13.9[\alpha_E(75^\circ)/\alpha_E(45^\circ)]^2. \quad (8)$$

In the absence of refraction, Eq. (8) predicts that the relative intensity of the peak from the Λ_1 band should be 13.9 times greater at $\psi=75^\circ$ than at $\psi=45^\circ$, a result which is independent of ξ_d or the position of the DTP. Experimentally, however, it is observed to be only between 2 and 3 times greater.

Several workers have attributed the peak observed near the Fermi level in the experimental spectra in Fig. 1 to emission from a surface state.^{16,4} It has been pointed out, however,¹¹ that rather than being due to a surface state, this peak might result from indirect transitions from the p -like states which have a high density near the Λ_1 band edge at L . The dashed theoretical curve was computed with $\Gamma=0.1(2\pi/a)$, $\alpha_p=6.0$, and $\alpha_E=0.19$. A peak near the Fermi level is indeed observed at -0.75 eV. However, this value for Γ is more than 3 times that which would be expected from the mean free path Λ_e through the result $\Gamma=1/2\Lambda_e$ ($\Lambda_e \approx 10$ Å); the peak shape is not in good agreement with experiment, possessing a low-energy tail which is not observed; and a value of 6.0 for α_p implies, for example, that the photoexcitation cross section for p_x and p_y states is more than 10 times larger than the cross section for d_{xz} and d_{yz} states (see I). The latter is not supported by first-principles calculations,¹² and, in addition, is in large disagreement with the results we obtained by choosing α_p so as to reproduce the intensities of peaks that are unquestionably from bulk s - p bands. We therefore rule out the indirect-transition interpretation of this peak.

2. $\hbar\omega=11.8$ eV, $\theta=35^\circ$, $\phi=0^\circ$

For $\phi=0^\circ$ (or 60°), the emission direction lies in the $GLUK$ mirror plane of the Brillouin zone (BZ), and the initial states sampled are thus of definite parity with respect to reflection in the plane containing the emission direction and the wave vector of the incident light. As discussed by Hermanson,²² transitions from the even (odd) symmetry states can be excited only by p - (s -) polarized light.

Figure 2 shows calculated and experimental spectra for

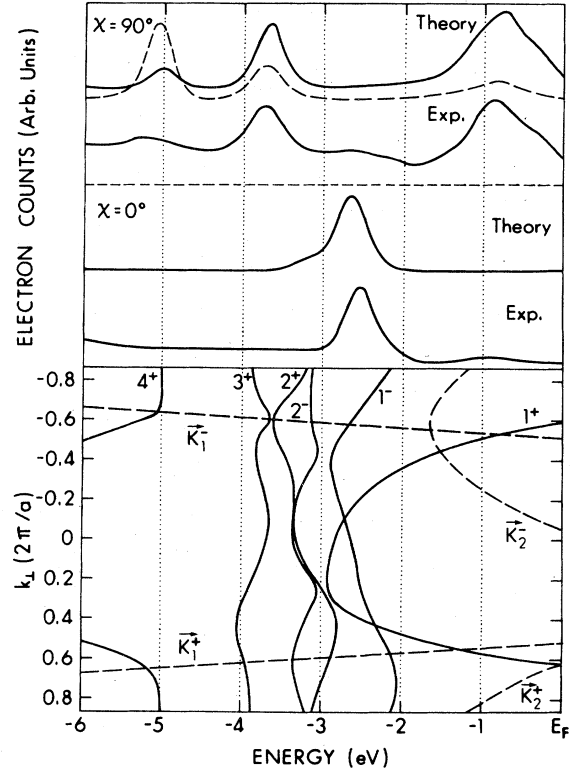


FIG. 2. Calculated and experimental ARP spectra for $\hbar\omega=11.8$ eV, $\theta=35^\circ$, $\phi=0^\circ$, and $\psi=55^\circ$. The dashed curve was computed with $\alpha_p=\alpha_s=0$.

$\chi=90^\circ$ and 0° . An interesting feature of the experimental spectrum for $\chi=90^\circ$ is that it contains a large contribution from the s - p component of the initial states. The dashed theoretical curve was computed with

$$\psi^f(\vec{r}) = e^{-0.03z} \langle \vec{r} | \text{OPW}(\vec{K}_1^-) \rangle, \quad (9)$$

and, to block out any contribution from the initial-state s - p component, $\alpha_p=\alpha_s=0$. Large disagreement with the experimental peak intensities is obtained. However, band 1^+ is 59% s - p -like and band 4^+ is 53% s - p -like at their respective DTP's for $|\text{OPW}(\vec{K}_1^-)\rangle$. Nonzero values of α_p and/or α_s increase the total photocurrent from one band while decreasing the total photocurrent from the other band. The solid theoretical curve was computed with the values of α_p and α_s quoted in Sec. III A, and reasonably good agreement with the experimental peak intensities is obtained.

In the spectrum for $\chi=0^\circ$, the predicted position of the peak from band 1^- is 0.1 eV too low, while a shoulder from band 2^- is predicted to occur at -3.2 eV but is not observed experimentally. However, the dispersions of bands 1^- and 2^- , and the variation with k_{\perp} of the optical matrix elements, are such that both of these discrepancies are removed by decreasing Φ so as to shift the position of the DTP $\approx 0.05(2\pi/a)$ to smaller k_{\perp} . We thus cannot conclude that the calculated positions of bands 1^- and/or 2^- are necessarily in error.

In the spectrum for $\chi=90^\circ$, bands 2^+ and 3^+ both contribute to the peak at -3.75 eV. Their average position,

at least, appears to be correct to within ≈ 0.1 eV. The position of the peak from band 1^+ is accurately predicted. However, since band 1^+ has a very high dispersion, the calculated peak position is very sensitive to Φ , and the band position can thus not be very precisely determined. Nevertheless, the successful prediction of the relative intensity, width, and shape of the peak from this band is strong evidence that the final state given by Eq.(9) is fairly accurate. In particular, the large peak width and the shoulder at -0.4 eV can be attributed to indirect transitions from states on band 1^+ for $-0.6 \leq k_{\perp} \leq -0.45(2\pi/a)$. This interpretation is opposed to that of Grepstad and Slagsvold.²³ From a study of the θ dependence of the position of the peak and shoulder from band 1^+ for $\hbar\omega=11.8$ eV, these authors concluded that these features were due to direct transitions to two different bulklike final-state bands, which, at $\theta=35^\circ$, are strongly hybridized, with dispersions which depart greatly from free-electron-like behavior.

$$3. \hbar\omega=11.8 \text{ eV}, \theta=75^\circ, \phi=0^\circ$$

For this emission angle and photon energy, we find that the final state cannot be adequately approximated by a single OPW. Figure 3 shows calculated and experimental spectra for $\chi=0^\circ$ and 90° . In the experimental spectrum for $\chi=90^\circ$, a very broad structure is observed between -2 and -4 eV, which would appear to originate entirely from band 2^+ . We show as the dashed curve a spectrum computed with

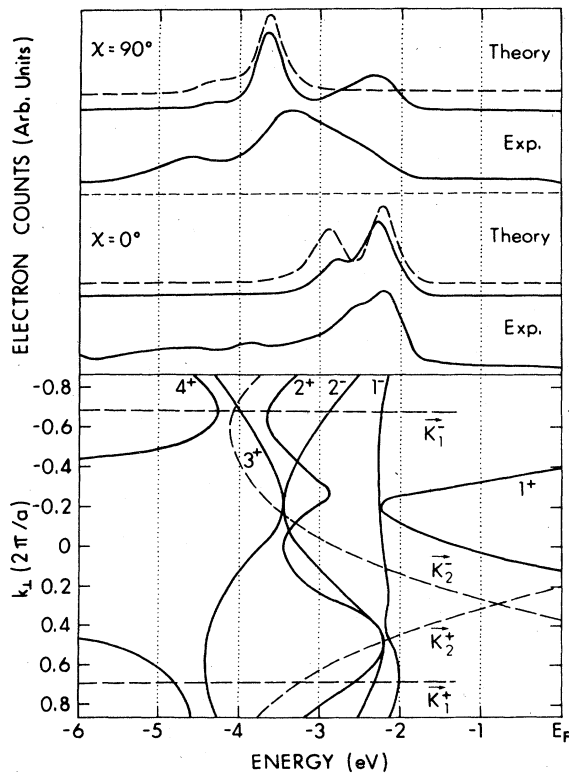


FIG. 3. Calculated and experimental ARP spectra for $\hbar\omega=11.8$ eV, $\theta=75^\circ$, $\phi=0^\circ$, and $\psi=15^\circ$. The solid theoretical curves were computed with a two-OPW final state.

$$\psi^f(\vec{r})=e^{-0.04z}\langle\vec{r}|\text{OPW}(\vec{K}_1^-)\rangle. \quad (10)$$

It is in large disagreement with experiment, containing only a single, relatively narrow, peak from band 2^+ , at -3.6 eV. The predicted photocurrent from initial states with energies approximately greater than -3 eV essentially vanishes. Including $|\text{OPW}(\vec{K}_2^+)\rangle$ in ψ^f produces a narrow peak at -2.2 eV, since the corresponding DTP lies on a critical point. Including $|\text{OPW}(\vec{K}_2^-)\rangle$ in ψ^f produces a peak at -3.3 eV. In order to account for the photocurrent observed in the region near -2.7 eV it is thus necessary to assume that $|\text{OPW}(\vec{K}_1^+)\rangle$ has a substantial amplitude in ψ^f . The solid theoretical curve was computed with

$$\psi^f(\vec{r})=e^{-0.04z}\{\langle\vec{r}|\text{OPW}(\vec{K}_1^-)\rangle + 1.5ie^{-0.06z}\langle\vec{r}|\text{OPW}(\vec{K}_1^+)\rangle\}. \quad (11)$$

There is still serious disagreement with experiment, as the position of the low energy peak is 0.3 eV too low and there is not nearly sufficient intensity in the region between the two peaks. It is not possible to remove the latter discrepancy by trying to increase the photocurrent from states on band 2^+ near the zone boundary by increasing the momentum broadening, since this instead has the predominant effect of increasing the photocurrent from states near the critical point at $k_{\perp}=0.5(2\pi/a)$. However, the large dispersion of band 2^+ suggests that the agreement between theory and experiment might be improved if the DTP's for $|\text{OPW}(\vec{K}_1^-)\rangle$ and $|\text{OPW}(\vec{K}_1^+)\rangle$ were closer to the zone boundary. Figure 4 shows the calculated spectrum for $\Phi=9.2$ eV and

$$\psi^f(\vec{r})=e^{-0.06z}\{\langle\vec{r}|\text{OPW}(\vec{K}_1^-)\rangle + 0.8i\langle\vec{r}|\text{OPW}(\vec{K}_1^+)\rangle\}. \quad (12)$$

With this value for the inner potential, the relatively large degree of momentum broadening resulting from a value for Γ of $0.06(2\pi/a)$ has the effect of producing a very broad structure resembling the one seen experimentally.

Note that, as was the case for $\theta=35^\circ$, the bulk bands at the relevant final-state energies will be strongly hybridized.

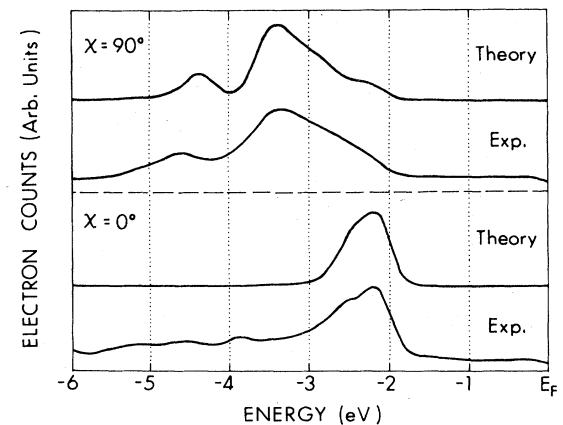


FIG. 4. Calculated and experimental ARP spectra for $\hbar\omega=11.8$ eV, $\theta=75^\circ$, $\phi=0^\circ$, and $\psi=15^\circ$.

dized, implying that Eq. (12) cannot be expressed as a linear combination of bulk bands, and thus that the experimental spectrum cannot be interpreted in terms of transitions to bulk states.

Comparing the theoretical and experimental spectra in Fig. 4, it is evident that the calculated position of band 4^+ is ≈ 0.25 eV too high. When ψ^f is determined by fitting to the experimental spectrum for $\chi=0^\circ$, similar results are obtained. In the spectrum calculated with the single-OPW final state of Eq. (10) (Fig. 3), the peak from band 2^- occurs at -2.9 eV, 0.4 eV lower than the position of the shoulder observed experimentally. When $|\text{OPW}(\vec{K}_1^+)|$ is included in ψ^f via Eq. (11), the peak shape agrees better with experiment, but the peak position still occurs at too low an energy. However, with ψ^f given by Eq. (12) and an inner potential Φ of 9.2 eV, agreement is obtained to within ≈ 0.1 eV.

4. $\hbar\omega = 11.8$ eV, $\theta = 55^\circ$, $\phi = 0^\circ$

Figure 5 shows calculated and experimental spectra for $\chi=0^\circ$ and 90° . Spectra computed with

$$\psi^f(\vec{r}) = e^{-0.04z} \langle \vec{r} | \text{OPW}(\vec{K}_1^-) \rangle \quad (13)$$

(and with $\Phi = 12.5$ eV) are shown as the dashed curves. For $\chi=0^\circ$, a peak is predicted to occur at -2.95 eV, but is not observed experimentally, while shoulders at -2.1 and -2.65 eV are observed in experiment but are not predicted. Decreasing Φ in the calculation shifts the posi-

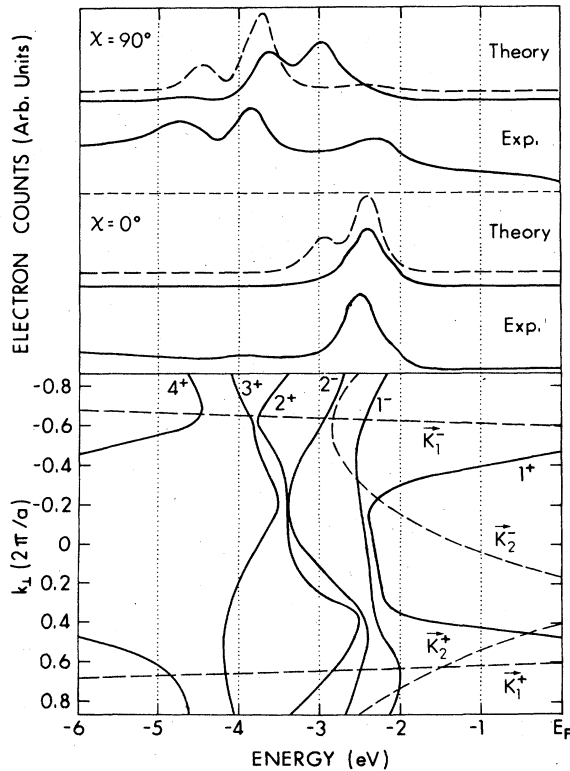


FIG. 5. Calculated and experimental ARP spectra for $\hbar\omega = 11.8$ eV, $\theta = 55^\circ$, $\phi = 0^\circ$, and $\psi = 35^\circ$. The solid theoretical curves were computed with a two-OPW final state.

tion of the peak at -2.95 eV to higher energies, and, since the relative amplitude of the optical transition matrix elements for states on band 2^- is smaller for smaller k_\perp , lowers its relative intensity. However, there is no value of Φ for which a peak-shoulder combination resembling the one seen experimentally between -2.4 and -2.7 eV is predicted, or for which a shoulder near -2.1 eV appears. The solid theoretical curves were computed with

$$\psi^f(\vec{r}) = e^{-0.04z} [\langle \vec{r} | \text{OPW}(\vec{K}_1^-) \rangle + 1.2e^{-i(3\pi/4)-0.03z} \times \langle \vec{r} | \text{OPW}(\vec{K}_1^+) \rangle], \quad (14)$$

and with $\Phi = 11.0$ eV so that the DTP's for both OPW's lie $0.06(2\pi/a)$ closer to the zone boundary than shown in Fig. 5. Reasonably good agreement is obtained for $\chi=0^\circ$. The peak predicted to occur at -2.45 eV actually represents two unresolved peaks, one from states on band 1^- near $k_\perp = -0.7(2\pi/a)$ and one from states on band 2^- near $k_\perp = 0.7(2\pi/a)$. The shoulder at -2.65 eV is from states on band 2^- near the BZ boundary. The agreement achieved with the final state of Eq. (14) suggests that the calculated positions of bands 1^- and 2^- at the relevant k_\perp are correct to within ≈ 0.1 eV.

It might appear from Fig. 5 that an alternative means of improving the agreement with a single-OPW final state could involve including $|\text{OPW}(\vec{K}_2^+)|$ in ψ^f . However, this causes there to be a large peak near the Fermi level in the calculated spectrum for $\chi=90^\circ$, and there is no trace of such a peak experimentally.

In the experimental spectrum for $\chi=90^\circ$, a rather broad peak is observed at -2.3 eV, with a peak height (after background subtraction) that is roughly $\frac{3}{5}$ that of the peak at -3.85 eV. In the calculation, this feature is not reproduced with a single-OPW final state (dashed curve), the two-OPW final state of Eq. (14), or any other final state of the form of Eq. (3), suggesting that there is a substantial error in the initial-state band structure. The source of this unusually large error can be understood by noticing from Figs. 2, 3, and 5 that the dispersion of band 2^+ for positive k_\perp is changing very rapidly as a function of k_\parallel . If band 2^+ had the same position for $\theta = 55^\circ$ that it has for the somewhat greater value of k_\parallel corresponding to $\theta = 75^\circ$ (Fig. 3), then the band energy at the DTP for $|\text{OPW}(\vec{K}_1^+)|$ would be 0.45 eV higher. Furthermore, the DTP would lie near a critical point at -2.25 eV, which would tend to cause the peak position to occur at an energy higher than the band energy at the DTP. Under these circumstances, a final state given by Eq. (14) could yield good agreement with experiment. As evidence of this, compare the experimental spectrum for initial-state energies greater than -4 eV with the solid theoretical curve, computed with a two-OPW final state, shown in Fig. 3 for $\chi=90^\circ$. We conclude, therefore, that the large disagreement is due to the failure of the combined interpolation scheme Hamiltonian to accurately describe the rapid variation in the dispersion of band 2^+ as a function of k_\parallel , and that the actual position of band 2^+ near $k_\perp = 0.63(2\pi/a)$ is in the neighborhood of -2.5 eV.

The calculated position of the peak from states on band

2^+ near $k_{\perp} = -0.7(2\pi/a)$ is sensitive to Φ ; however, the band position is evidently 0.1–0.2 eV too high. It is difficult to place band 4^+ by comparing the theoretical and experimental spectra because of the high sensitivity of the calculated photocurrent on the final-state parameters.

$$5. \hbar\omega = 21.2 \text{ eV}, \theta = 80^\circ, \phi = 0^\circ$$

For this photon energy and emission angle our model for ψ^f contains up to eight OPW's. Figure 6 shows an experimental spectrum obtained with unpolarized light. The theoretical curve was computed with

$$\psi^f(\vec{r}) = e^{-0.04z} \langle \vec{r} | \text{OPW}(\vec{K}_1^-) \rangle. \quad (15)$$

Since the agreement with experiment is very poor, it is evident that $|\text{OPW}(\vec{K}_1^-)\rangle$ has a particularly small amplitude in ψ^f for this emission angle and photon energy. Nine separate peaks and shoulders can be identified in the experimental spectrum, suggesting that several OPW's may have significant amplitudes in ψ^f . Allowing all eight OPW amplitudes to be nonzero, however, would introduce too many parameters to make any final-state determination meaningful.

$$6. \hbar\omega = 16.9 \text{ eV}, \theta = 45^\circ, \phi = 30^\circ$$

For $\phi = 30^\circ$, the emission direction lies in the ΓLW plane of the BZ. Unlike the case for $\phi = 0^\circ$ and 60° , there are in general no symmetry forbidden optical transitions. Figure 7 shows an experimental spectrum for $\chi = 90^\circ$,

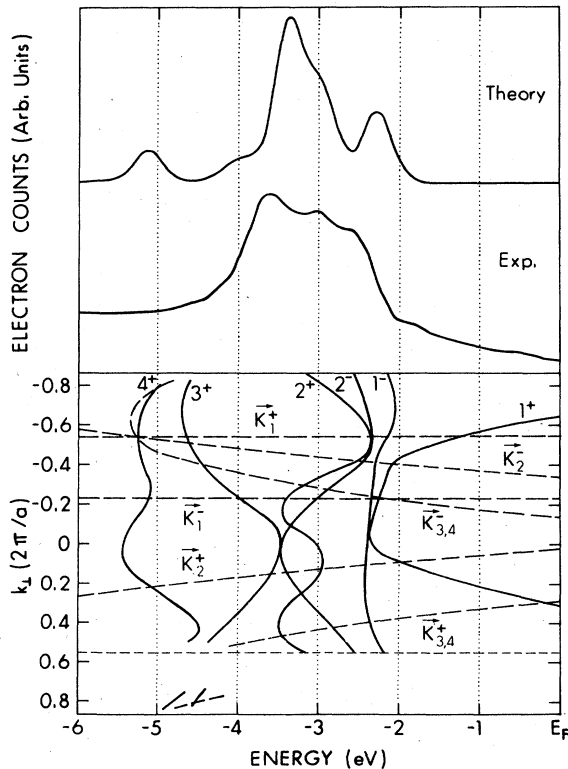


FIG. 6. Calculated and experimental ARP spectra for $\hbar\omega = 21.2 \text{ eV}$, $\theta = 80^\circ$, $\phi = 0^\circ$, $\psi = 45^\circ$, and unpolarized light.

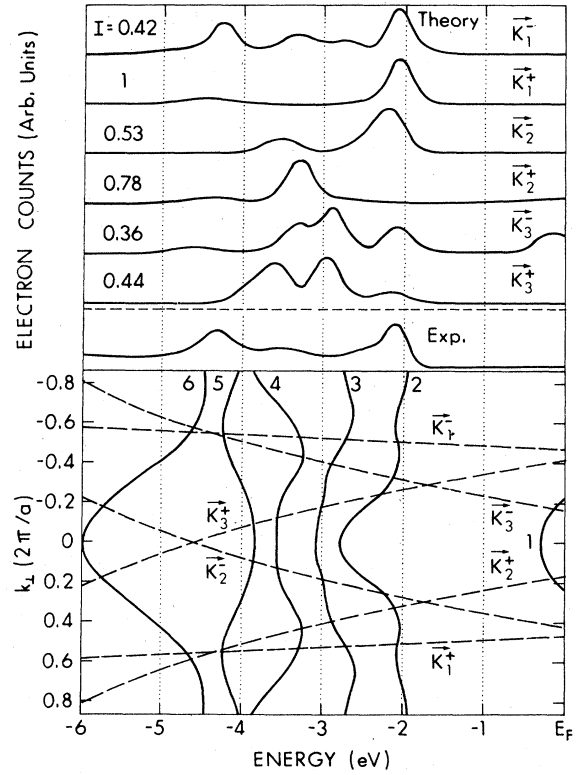


FIG. 7. Calculated and experimental ARP spectra for $\hbar\omega = 16.9 \text{ eV}$, $\theta = 45^\circ$, $\phi = 30^\circ$, $\chi = 90^\circ$, and $\psi = 45^\circ$.

along with theoretical spectra computed with the six possible final states of the form

$$\psi^f(\vec{r}) = e^{-0.04z} \langle \vec{r} | \text{OPW}(\vec{K}_n^\pm) \rangle. \quad (16)$$

The quantity I gives the relative height of the largest peak in the spectrum. Comparison of the theoretical and experimental curves suggests that only $|\text{OPW}(\vec{K}_1^-)\rangle$ has a significant amplitude in ψ^f . The agreement obtained indicates that the calculated positions of bands 2 and 5 are correct to within 0.1 eV, while the calculated positions of bands 3 and 4 are correct to within 0.2 eV.

$$7. \hbar\omega = 21.2 \text{ eV}, \theta = 20^\circ, \phi = 60^\circ$$

Figure 8 shows an experimental spectrum obtained with unpolarized light, and a theoretical spectrum computed with

$$\psi^f(\vec{r}) = e^{-0.03z} \langle \vec{r} | \text{OPW}(\vec{K}_1^-) \rangle. \quad (17)$$

Very good agreement with experiment is obtained, indicating that $|\text{OPW}(\vec{K}_1^-)\rangle$ dominates the final state. The relevant band positions appear correct to within 0.2 eV.

IV. DISCUSSION

Our main conclusion from the above results is that the final state in photoemission can be adequately described in terms of Eq. (3), with an \hat{R} - and E -dependent inner potential. In cases in which a one- or two-OPW wave function

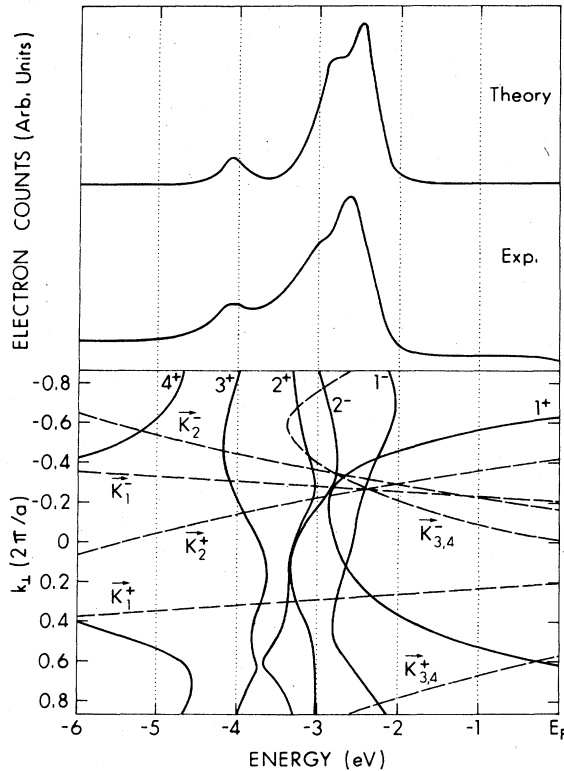


FIG. 8. Calculated and experimental ARP spectra for $\hbar\omega=21.2$ eV, $\theta=20^\circ$, $\phi=60^\circ$, $\psi=45^\circ$, and unpolarized light.

does not give good agreement with experiment, this conclusion is somewhat tentative. Although in such cases the presence of additional OPW's in Eq. (3) provides a plausible explanation for the observed disagreements, a comparison of calculated and experimental spectra becomes impractical due to the large number of final-state parameters.

In previous works, Shevchik and Liebowitz,²⁴ and Nilsson and Dahlbäck,⁷ have argued on theoretical grounds that final-state damping could result in final-state bands which exhibit free-electron-like behavior, and our results clearly support this idea. The interpretation of spectra in terms of bulk final-state bands is thus acceptable only when these bands have free-electron-like dispersions. Even in this case, however, small errors may be introduced from a displacement in k_{\perp} of the actual band from the bulk band. In disagreement with these considerations, Dietz and Himpsel²⁵ recently studied the dependence of peak position on photon energy in normal emission spectra obtained from a Cu(110) surface for $\hbar\omega$ near 18 eV, and concluded that the observation of a plateau in the peak position as the photon energy was increased, so as to bring the final-state energy into a band gap at X , ruled out a free-electron-like behavior for the final state. This conclusion is unjustified, however, as momentum broadening can cause a peak to occur at the energy corresponding to the high one-dimensional density of initial states at X , even when the final state is displaced somewhat in k_{\perp} from X .

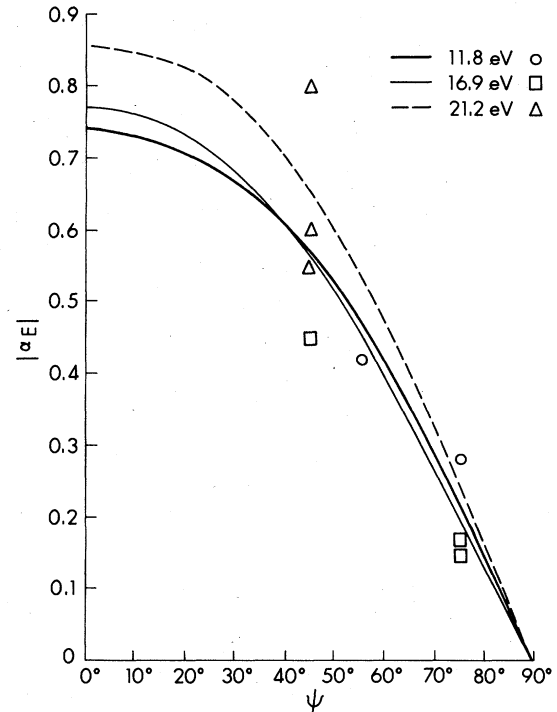


FIG. 9. Comparison of the experimentally determined values for $|\alpha_E(\psi)|$ with the predictions of the Fresnel equations.

Mixing of OPW's in the final state, variation in the effective inner potential, and the sometimes large effects of momentum broadening, all introduce inaccuracies in any simple prescription for extracting band positions directly from ARP spectra. This applies as well to the so-called "absolute" triangulation methods. The scheme presented in I is useful in identifying such effects and arriving at a band-structure analysis which is consistent with inherent uncertainties in the final-state wave function.

Finally, we turn to a discussion of the results found concerning the refraction of the incident electric field at the surface. In Fig. 9 the predictions of the macroscopic Maxwell equations for $\alpha_E(\psi)$ are plotted for photon energies of 11.8, 16.9, and 21.2 eV. The optical constants for Cu at these energies are given by Ehrenreich and Philipp.²⁶ Also plotted are the values of $\alpha_E(\psi)$ used in the calculation of spectra. Values corresponding to spectra which were not very sensitive to its value are not included. Allowing for the uncertainties involved in fitting $\alpha_E(\psi)$ to experiment with a completely parametrized scheme, we do not find large disagreements between the experimental values and those predicted by the Fresnel equations. This disagrees with Smith *et al.*'s results.¹⁹ They found, for example, that in order to reproduce the experimental peak intensities in a spectrum obtained with $\hbar\omega=10.5$ eV at normal emission from Cu(111), a value $\alpha_E (= \sqrt{\epsilon})$, in the notation of Ref. 19) of 0.16 had to be used, for light incident at 60° . For $\hbar\omega=10.5$ eV and $\psi=60^\circ$, the value for α_E predicted by the Fresnel equations is 0.42, approximately $2\frac{1}{2}$ times greater.

ACKNOWLEDGMENTS

I wish to gratefully acknowledge the support and guidance of Franco Jona while this work was carried out and many invaluable discussions with P. B. Allen and J. W.

Davenport. The assistance of D. Liebowitz and N. J. Shevchik with the experimental work is acknowledged. This work was supported in part by the National Science Foundation.

- *Present address: Department of Chemistry, University of Hawaii at Manoa, Honolulu, HI 96822.
- ¹J. Stöhr, P. S. Wehner, R. S. Williams, G. Apai, and D. A. Shirley, *Phys. Rev. B* **17**, 587 (1978).
- ²P. Thiry, D. Chandesris, J. Lecante, C. Guillot, R. Pinchaux, and Y. Pétrouff, *Phys. Rev. Lett.* **43**, 82 (1979).
- ³M. Pessa, M. Lindroos, and R. Lindström, *Solid State Commun.* **32**, 585 (1979).
- ⁴J. A. Knapp, F. J. Himpsel, and D. E. Eastman, *Phys. Rev. B* **19**, 4952 (1979).
- ⁵M. Lindroos, H. Asonen, M. Pessa, and N. V. Smith, *Solid State Commun.* **39**, 285 (1981).
- ⁶M. Pessa, M. Lindroos, H. Asonen, and N. V. Smith, *Phys. Rev. B* **25**, 738 (1982).
- ⁷P. O. Nilsson and N. Dahlbäck, *Solid State Commun.* **29**, 303 (1979).
- ⁸N. J. Shevchik, *J. Electron Spectrosc. Relat. Phenom.* **14**, 411 (1978).
- ⁹J. A. R. Samson, *Techniques of Vacuum Ultraviolet Spectroscopy* (Wiley, New York, 1967), p. 300.
- ¹⁰D. Liebowitz, M. Sagurton, J. Colbert, and N. J. Shevchik, *Phys. Rev. Lett.* **39**, 1625 (1977).
- ¹¹M. Sagurton and N. J. Shevchik, *Phys. Rev. B* **17**, 3859 (1978).
- ¹²D. W. Jepsen, *Phys. Rev. B* **20**, 402 (1979).
- ¹³G. A. Burdick, *Phys. Rev.* **129**, 138 (1963).
- ¹⁴N. V. Smith and L. F. Mattheiss, *Phys. Rev. B* **9**, 1341 (1974).
- ¹⁵H. Becker, E. Dietz, U. Gerhardt, and H. Angermüller, *Phys. Rev. B* **12**, 2084 (1975).
- ¹⁶P. O. Gartland and B. J. Slagsvold, *Phys. Rev. B* **12**, 4047 (1975).
- ¹⁷E. Dietz, H. Becker, and U. Gerhardt, *Phys. Rev. Lett.* **36**, 1397 (1976); **37**, 115 (1976).
- ¹⁸L. F. Wagner, Z. Hussain, and C. S. Fadley, *Solid State Commun.* **21**, 257 (1977).
- ¹⁹N. V. Smith, R. L. Benbow, and Z. Hurych, *Phys. Rev. B* **21**, 4331 (1980).
- ²⁰S. Holloway, D. E. Grider, and J. K. Sass, *Solid State Commun.* **39**, 953 (1981).
- ²¹J. F. Janak, A. R. Williams, and V. L. Moruzzi, *Phys. Rev. B* **11**, 1522 (1975).
- ²²J. Hermanson, *Solid State Commun.* **22**, 9 (1977).
- ²³J. K. Grepstad and B. J. Slagsvold, *Solid State Commun.* **34**, 821 (1980).
- ²⁴N. J. Shevchik and D. Liebowitz, *Phys. Rev. B* **18**, 1618 (1978).
- ²⁵E. Dietz and F. J. Himpsel, *Solid State Commun.* **30**, 235 (1979).
- ²⁶H. Ehrenreich and H. R. Philipp, *Phys. Rev.* **128**, 1622 (1962).